VIA MEDICA

ORIGINAL ARTICLE

Folia Morphol.
Vol. 68, No. 2, pp. 70–78

ISSN 0015–5659
www.fm.viamedica.pl

A morphometric comparative study of the lateral geniculate body in selected placental mammals: the common shrew, the bank vole, the rabbit, and the fox

J. Najdzion, B. Wasilewska, K. Bogus-Nowakowska, M. Równiak, S. Szteyn, A. Robak

Department of Comparative Anatomy, University of Warmia and Mazury, Olsztyn, Poland

[Received 8 September 2008; Accepted 8 April 2009]

The lateral geniculate body (LGN) was morphometrically examined and compared in representatives of four mammalian orders (Insectivora, Rodentia, Lagomorpha, and Carnivora). In each studied species, the lateral geniculate body was divided into two distinct parts: the dorsal nucleus (LGNd) and the ventral nucleus (LGNv). The lateral geniculate body of the common shrew and the bank vole are very similar in appearance and nuclear pattern. The dorsal and ventral nuclei of these two species also have the most similar statistical characteristics. The lateral geniculate body of the fox has the most complicated morphology and multilayered structure. A significant disproportion was observed between the sizes of both geniculate nuclei in the fox, where the dorsal nucleus definitely surpassed the ventral nucleus in terms of volume. With the exception of the fox, the neuronal density of the LGN nuclei was negatively correlated with the volumes of the LGN. The mean neuronal size of the LGNd and LGNv, which was the resultant of the length, width, area, and circumference of the soma, grew correlatively to the volumes of these nuclei. In all examined species, somas of the LGNd neurons are distinctly larger and have more similar shapes than the LGNv perikarya. In addition, the numerical density of neurons in the ventral nucleus is significantly higher than in the dorsal nucleus. All these morphometric parameters clearly differentiate the LGNd from the LGNv (Folia Morphol 2009; 68, 2: 70–78).

Key words: lateral geniculate body, morphometric analysis

INTRODUCTION

The lateral geniculate body (LGN) of mammals forms an oval protrusion at the lateral edge of the thalamus. The LGN is not a homogeneous structure, since it is separated into two main divisions: the dorsal nucleus (LGNd) and the ventral nucleus (LGNv). The small third division, located between the LGNd and the LGNv, was described as the intergeniculate leaflet (IGL) by Hickey and Spear [13]. The LGNv and IGL share many neurochemicals, projections, and physiological properties. Therefore, some authors do not identify the IGL as a separate part of the LGN, but as a subdivision of the LGNv [11]. Each of the nuclei of the LGN has a different function. The LGNd is the thalamic relay centre that processes visual information on its way from the retina to the primary visual cortex [21]. The IGL, similarly to the LGNd, receives direct binocular retinal input. The central circadian pacemaker in mammals is located in the suprachiasmatic nucleus (SCN) of the hypo-

Address for correspondence: J. Najdzion, Department of Comparative Anatomy, University of Warmia and Mazury, Plac Łódzki 3, 10–727 Olsztyn, Poland, e-mail: jnajdzion@uwm.edu.pl

thalamus. Photic information is transmitted to the SCN directly from the retina via the retinohypothalamic tract, and indirectly from the IGL via the geniculohypothalamic tract [8]. The IGL also receives nonphotic input from other brain areas and it is thought to modulate and integrate photic and nonphotic entrainment of circadian rhythms in mammals [10, 28]. The LGNv does not project to the cortex, but it has connections with many subcortical visual, as well as nonvisual, structures [6]. While the connections of the LGNv have been extensively characterised, little is known about the function of this structure. The projections of the LGNv suggest that this nucleus participates in visuosensory and visuomotor functions such as brightness discrimination, saccade eye movement, and pupillary light reflex [6]. Thus, it may play a role as an integrative component of the visual and ocular motor systems [17, 18]. Behavioural and immunocytochemical studies suggest that the LGNv, similarly to the IGL, plays a major role in mediating photic and nonphotic phase shifts of circadian rhythms [11].

Although literature on the LGN seems to be abundant, a complex comparative morphometric study of the LGN nuclei in different mammalian species has not been carried out. Our goal was to characterize the LGN subdivisions and their neurons in terms of morphometric attributes. In the present study the LGN of representatives of four different placental mammalian orders were morphometrically compared.

MATERIAL AND METHODS

The study was performed on 20 brains from 4 species: the common shrew (Sorex araneus — Insectivora), the bank vole (Clethrionomys glareolus — Rodentia), the rabbit (Oryctolagus cuniculus — Lagomorpha), the fox (Vulpes vulpes — Carnivora). Each species was represented by 5 adult specimens of both sexes of the following body weight: the common shrew 11–12 g, the bank vole 19–24 g, the rabbit 3.5–4.5 kg, and the fox 8–10 kg. The first 2 species were wild-living animals that were caught with the permission of the Polish Environment Ministry (permission number: DLOPiKog.4201\262\00). The remaining 2 species were bred animals obtained from commercial sources: the Vienna Blue rabbit and the silver fox. All efforts were made to minimize animal suffering and to use only the number of animals necessary to produce reliable scientific data. The surgical procedures followed the guidelines established by the Animal Care and Use Ethical Committee of the University of Warmia and Mazury. All animals were given a lethal dose of Nembutal (80 mg/kg) intraperitoneally and then were decapitated. The brains were removed from the skulls and immediately placed into 10% buffered formalin for immersion fixation for at least 2 months. In the cases of the rabbit and fox, the brains were cut into two sagittal halves before being placed in fixative. After the fixation, all the brains were dehydrated in a graded series of ethanols and embedded in paraffin. Next, they were coronally cut on a microtome (Leica, Germany) into serial 50 μm sections and then stained with cresyl violet. Nissl staining was chosen as the best quantitative method for measuring cells, since it stains all perikarya nonspecifically. All sections were analysed cytoarchitectonically (to define the boundaries of the LGN) and morphometrically with a calibrated image analysis system that consisted of a computer equipped with morphometric software (Multi-Scan 8.2, Computer Scanning Systems, Poland) and a light microscope coupled with a digital camera (CM40P, VideoTronic, Germany). The brain of each single animal was treated identically in accordance with the following standardized procedure:

Computer reconstructions of the lateral geniculate body

Partial microscopic images (512 × 512 pixel size) of single brain sections were digitally recorded by means of a camera attached to a microscope and a computer. All recorded images were combined in one large digital section that represented the whole LGN and the adjoining structures. In order to obtain as exact corresponding brain areas as possible, every section in the series of histological preparations was digitally reconstructed and stored in the form of computer images.

Volumetric analysis

The total volume of the LGN and its individual nuclei were calculated according to the formula proposed by DeVito et al. [7], in which the total volume of a structure (V_0) is the sum of the subvolumes of sections through the structure (V_n):

$$V_0 = \Sigma V_n$$

The subvolumes (V_n) were calculated by the formula:

$$V_n = \frac{Z_n}{3} \times (A_n + A_{n+1} + \sqrt{A_n \times A_{n+1}})$$

where: A_n — is the area of the examined structure on the n^{th} section; A_{n+1} — is the area of the examined structure on the $(n+1)^{th}$ section; Z_n — is the distance between the two sections.

The subvolumes of extreme sections (the rostral and caudal poles) were estimated by the formula:

$$V_n = \frac{Z_n}{3} \times (A_n)$$

On the examined digital sections, the boundaries of the individual geniculate nuclei were outlined by a mouse-driven cursor, and their areas were calculated by computer with morphometric software (Multi-Scan 8.2). To obtain the most accurate total volume, each digital section in the series was sampled.

Estimation of numerical density

The numerical density of the cells in each of the LGN nuclei was estimated using the optical dissector method described in details by West and Gundersen [29].

Estimation of the total number of neurons

The total number of neurons in each of the examined nuclei was calculated by multiplying estimates of the numerical density with the volume [29]:

$$N_0 = V_0 \times N_{mm}{}^3$$

where: V_0 — is the total volume of the examined structure and $N_{mm}{}^3$ — is the numerical density of this structure.

Morphometric parameters of the neurons

The morphometric parameters of the geniculate cells were measured and analyzed using a calibrated system and image-analyzing computer software (Multi-Scan 8.2). The morphometric analysis was performed with 40 × (fox, rabbit) and 100 × (common shrew, bank vole) objectives. The first section in the series was randomly selected, and then every second (common shrew, bank vole) and fifth (rabbit, fox) serial section was investigated for a single animal. All neurons with distinct nuclei were selected for analysis. The identified neuronal cells were digitally outlined and measured. The analyzed neuronal parameters were as follows: length (the long axis of the soma), width (the short axis of the soma), area of soma, circumference of soma, and shape factor (the ratio of both axes).

Statistical analysis

The statistical analysis was made using Statistica v.5.0 software (Statsoft, USA). All results were expressed as mean value ± standard error of the mean (SEM). Statistical evaluations of the differences between groups of data were performed using ANOVA followed by post-hoc Duncan's tests and paired Student's t-tests. The correlation coefficients (r) between several morphometric parameters were estimated. The significance level was set at $p < 0.05$.

RESULTS

The nuclear pattern of the lateral geniculate body

In all examined species, the LGN was clearly divided into two distinct parts: the dorsal nucleus (LGNd) and the ventral nucleus (LGNv). Since the boundaries of the intergeniculate leaflet were very difficult to define based on cytoarchitecture and the possible margin of error was too high, this structure was treated as part of the LGNv. The LGNs of the common shrew and the bank vole were very similar in appearance and nuclear pattern. In transverse sections, the LGNd and LGNv formed a crescent shape that was located at the lateral edge of the thalamus (Fig. 1A, B). The examined nuclei had a homogeneous structure, and no cytoarchitectonic lamination could be observed in either species, with the exception of the bank vole LGNv, which consisted of 2 poorly differentiated layers. Similar localization of the LGN was observed in the rabbit; however, the LGNd had a kidney shape and it was noticeably larger than the oval-shaped LGNv. In the middle section of the rabbit LGN, both nuclei could be subdivided into two parts (Fig. 2A), whereas the rostral and caudal poles of these structures were cytoarchitecturally uniform. The LGN of the fox had the most complicated nuclear pattern. In the rostrocaudal direction, the fox LGNd changed its shape from an oval to a C shape and then back to an oval (Fig. 2B, 3A, B). This structure comprised four cellular layers along almost its entire length, which seems to reflect the basic pattern of laminar organization of the carnivores LGNd. The small, spindle-shaped LGNv had a poorly delineated tripartite structure and it adjoined the LGNd ventrolaterally only in the rostral section (Fig. 2B).

Morphometric parameters of the lateral geniculate body

The morphometric data of the LGN and its nuclei are shown in Table 1 and Figures 4 and 5.

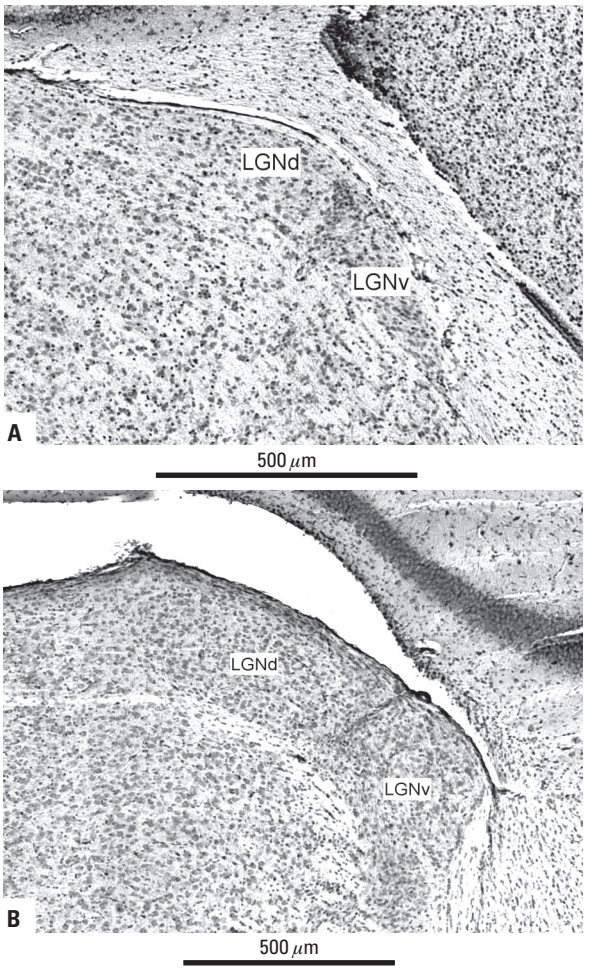

Figure 1. A. Transverse section of the common shrew lateral geniculate body; **B.** Transverse section of the bank vole lateral geniculate body; LGNd — dorsal nucleus of the lateral geniculate body; LGNv — ventral nucleus of the lateral geniculate body. Scale bar: 500 μm [22].

Volume

In the examined species, the volume of the LGNd ranged from 0.03 to 20 mm^3. The smallest volume was observed in the common shrew, and the largest volume was observed in the fox. The volume of the LGNv ranged between 0.02 and 3 mm^3. The smallest volume was also observed in the common shrew, but differently from the LGNd, the largest volume of the LGNv was noted in the rabbit. The contribution of the LGNd to the total volume of the LGN ranged from the lowest value of 57% in the bank vole to the largest, at 95%, in the fox. In case of the LGNv, the lowest percentage contribution of 5% was noted in the fox, while the largest, at 43%, was seen in the bank vole. The volumes and percentages of volumes were significantly different ($p < 0.05$) among the examined species, except for the volumetric percentages of the common shrew and bank vole, which did not differ significantly ($p > 0.34$).

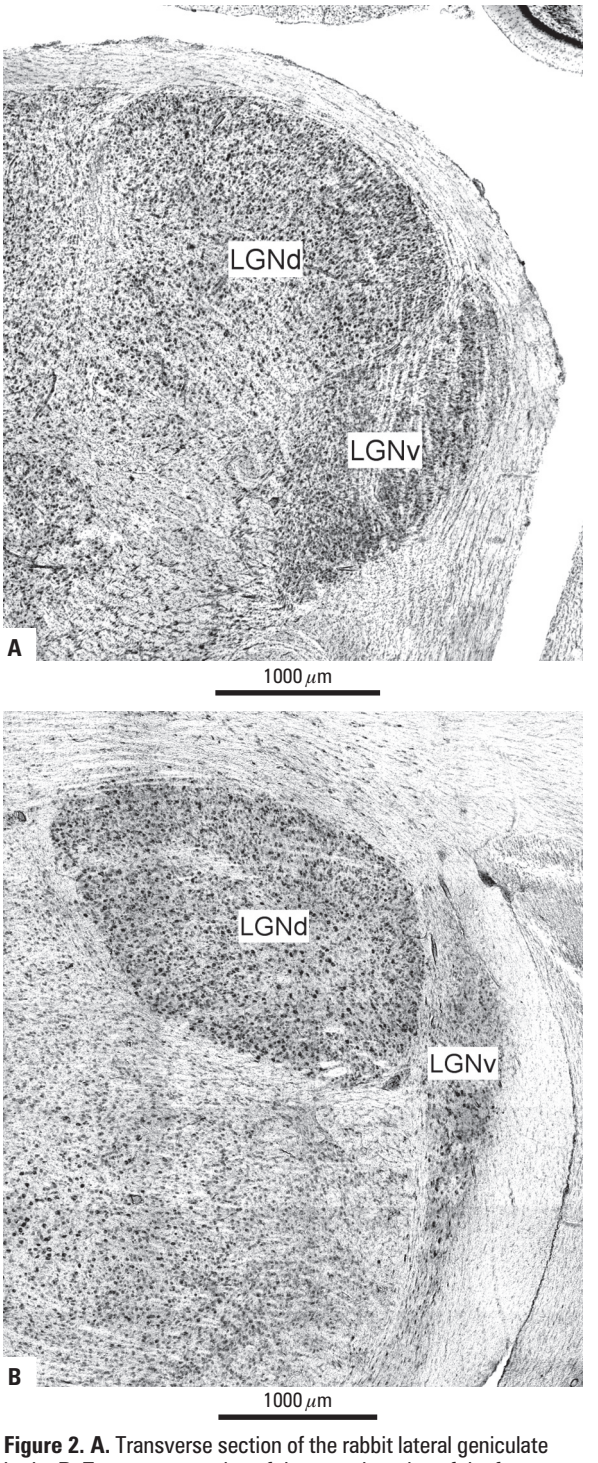

Figure 2. A. Transverse section of the rabbit lateral geniculate body; **B.** Transverse section of the rostral portion of the fox lateral geniculate body; LGNd — dorsal nucleus of the lateral geniculate body; LGNv — ventral nucleus of the lateral geniculate body. Scale bar: 1000 μm.

Numerical density

In each examined species, the LGNv was always characterized by a higher number of neurons per mm^3 than the LGNd. The numerical density of LGNd cells was lowest in the rabbit (26379 N/mm^3), while the highest was found in the common shrew

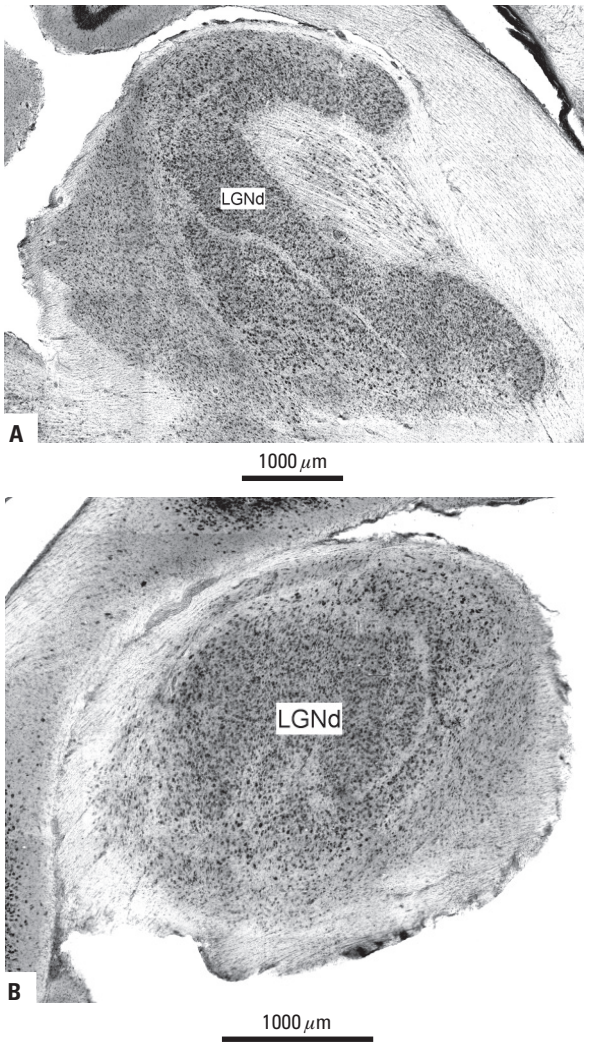

Figure 3. A. Transverse section of the middle portion of the fox lateral geniculate body; **B.** Transverse section of the caudal portion of the fox lateral geniculate body; LGNd — dorsal nucleus of the lateral geniculate body. Scale bar: 1000 μm.

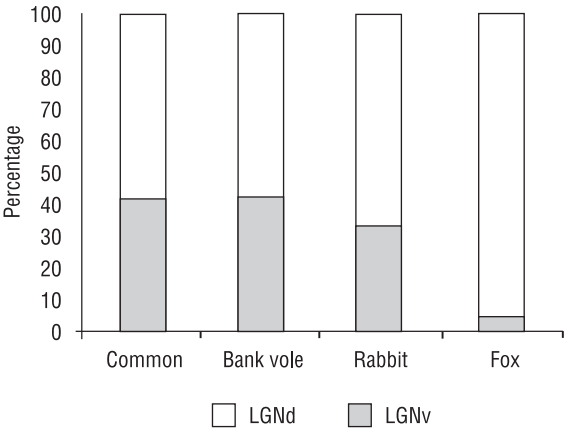

Figure 4. Percentages of dorsal nucleus of the lateral geniculate body (LGNd) and ventral nucleus of the lateral geniculate body (LGNv) volumes in the total lateral geniculate body volume.

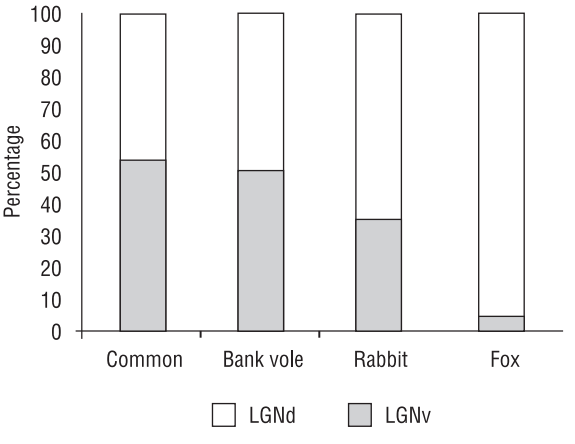

Figure 5. Percentages of dorsal nucleus of the lateral geniculate body (LGNd) and ventral nucleus of the lateral geniculate body (LGNv) neurons in the total number of lateral geniculate body neurons.

Table 1. Morphometric parameters of the lateral geniculate body (LGN); LGNd — dorsal nucleus of the lateral geniculate body; LGNv — ventral nucleus of the lateral geniculate body

	Common shrew	Bank vole	Rabbit	Fox
Volume of [mm^3]:				
LGN	0.05 ± 0.003	0.2 ± 0.01	9 ± 0.2	21 ± 0.4
LGNd	0.03 ± 0.002	0.1 ± 0.008	6 ± 0.1	20 ± 0.3
LGNv	0.02 ± 0.0005	0.09 ± 0.006	3 ± 0.09	1 ± 0.04
Density of [N/mm^3]:				
LGN	262158 ± 4934	186326 ± 6943	28112 ± 756	32493 ± 1188
LGNd	199009 ± 5956	153782 ± 4255	26379 ± 867	31183 ± 1067
LGNv	325306 ± 3911	218871 ± 9631	29845 ± 645	33804 ± 1309
Number of neurons (N):				
LGN	12029 ± 366	38779 ± 1378	248189 ± 4303	668941 ± 11074
LGNd	5580 ± 268	18907 ± 784	158449 ± 3392	633557 ± 10757
LGNv	6449 ± 98	19873 ± 593	89739 ± 910	35384 ± 318

(199009 N/mm^3). The mean neuronal densities of the LGNd in the common shrew and bank vole were significantly lower ($p < 0.05$) than the respective mean neuronal densities of the LGN in these species. In the case of the rabbit and fox, the mean numerical densities of the LGNd were not significantly different (rabbit: $p > 0.12$; fox: $p > 0.44$) from the respective mean numerical densities of the LGN. The neuronal density of the LGNd was negatively correlated with the volume of the LGNd ($r = –0.76$; $p < 0.24$). Similarly to the LGNd, the lowest neuronal density of the LGNv was observed in the rabbit (29845 N/mm^3), while the highest was seen in the common shrew (325306 N/mm^3). The mean neuronal densities of the LGNv in the common shrew and bank vole were significantly higher ($p < 0.05$) than the respective mean neuronal densities of the LGN in these species. As for the rabbit and fox, the mean numerical densities of the LGNv were not significantly different (rabbit: $p > 0.12$; fox: $p > 0.44$) from the respective mean numerical densities of the LGN. The neuronal density of the LGNv was negatively correlated with the volume of the LGNv ($r = –0.79$; $p < 0.21$).

Total number of neurons

In the present study, the smallest number of LGNd neurons was observed in the common shrew (5580), which accounted for 46%, while the largest was found in the fox (633557), which accounted for 95% of the total neuronal population. Among all the examined species, the mean percentage contributions of the LGNd cells to the total neuronal populations of the LGN were significantly different ($p < 0.05$). In case of LGNv, the lowest cell population was found in the common shrew (6449), whereas the largest was found in the rabbit (89739). The contribution of the LGNv to the total neuronal population of the LGN ranged from the lowest value of 5% in the fox to the highest value of 54% in the common shrew. Among all the examined species, the mean percentage contributions of the LGNv cells to the total neuronal populations of the LGN were also significantly different ($p < 0.05$). The volume of the LGN was positively correlated with the mean percentage contributions of the LGNd cells ($r = 0.99$; $p < 0.004$) and negatively correlated with the mean percentage contributions of the LGNv neurons ($r = –0.99$; $p < 0.004$). There was a correlation between the growth of LGNd volume and the increase of the mean neuronal population of LGNd ($r = 0.99$; $p < 0.002$). A similar correlation was observed in the case of LGNv ($r = 0.99$; $p < 0.01$).

Morphometric parameters of geniculate neurons

The morphometric parameters of the geniculate cells are shown in Table 2.

In the studied species, the LGNd and LGNv neurons were diverse in size and shape. In general, with regard to both geniculate nuclei, the smallest neurons were observed in the common shrew, while the largest were seen in the fox. Only the LGNv cells of the rabbit and fox were characterized by similar sizes. In all examined species, the morphometric size parameters of the LGNd were significantly larger ($p < 0.05$) than the respective mean neuronal sizes of the LGN, except for the fox, in which the neuronal length was not significantly different to the mean ($p > 0.52$). The mean sizes of the LGNv cells were significantly smaller ($p < 0.05$) than the respective mean sizes of the LGN neurons. A correlation was observed between the growth of the LGNd volume and the increase of the LGNd neuronal sizes (area of soma: $r = 0.88$; $p < 0.12$; circumference of soma: $r = 0.86$; $p < 0.14$; length: $r = 0.87$; $p < 0.13$; width: $r = 0.85$; $p < 0.15$). The sizes of the LGNv neurons grew correlatively with the increase of the LGNv volume as well ($r = 0.87$; $p < 0.13$; $r = 0.77$; $p < 0.23$; $r = 0.69$; $p < 0.31$; $r = 0.94$; $p < 0.06$, respectively).

The shape of the neuron can be expressed by the ratio of the length and width of the soma (shape factor). The smallest shape factor values of the LGNd were observed in the common shrew (1.44), while the largest was seen in the fox (1.53). In the rabbit and the fox, the mean shape factor values of LGNd were significantly lower ($p < 0.05$) than the respective mean shape factor values of LGN in these species. In the bank vole, this parameter was significantly higher ($p < 0.05$), while in the common shrew it was not significantly different ($p > 0.14$) from the respective means. The smallest shape factor values of the LGNv were found in the bank vole (1.40), whereas the largest was seen in the fox (2.12). Conversely to the LGNd, the mean shape factor values of the LGNv in the rabbit and the fox were significantly higher ($p < 0.05$), while in the bank vole, they were significantly lower ($p < 0.05$) than the respective means of the LGN. In the common shrew, the same parameter was not significantly different ($p > 0.23$) from the mean. There was a correlation between the volume of the LGNd and the shape factor value of the LGNd ($r = 0.87$; $p < 0.13$). In case of the LGNv, the similar correlation was weaker ($r = 0.17$; $p < 0.83$).

Table 2. Morphometric parameters of the lateral geniculate body (LGN) neurons; LGNd — dorsal nucleus of the lateral geniculate body; LGNv — ventral nucleus of the lateral geniculate body

	Common shrew	Bank vole	Rabbit	Fox
Area of soma [μm^2]:				
LGN	57 ± 6	72 ± 6	151 ± 7	157 ± 16
LGNd	67 ± 3	82 ± 5	166 ± 4	190 ± 1
LGNv	46 ± 2	63 ± 4	137 ± 1	124 ± 4
Circumference of soma [μm]:				
LGN	30 ± 2	33 ± 1	49 ± 1	52 ± 1
LGNd	33 ± 1	35 ± 1	51 ± 1	54 ± 0.2
LGNv	27 ± 1	30 ± 1	47 ± 0.3	49 ± 1
Length of soma [μm]:				
LGN	11 ± 0.5	12 ± 0.5	18 ± 0.3	20 ± 0.3
LGNd	12 ± 0.3	13 ± 0.2	18 ± 0.2	20 ± 0.1
LGNv	10 ± 0.2	11 ± 0.4	17 ± 0.2	19 ± 0.4
Width of soma [μm]:				
LGN	7 ± 0.4	8 ± 0.4	12 ± 0.4	11 ± 1
LGNd	8 ± 0.2	9 ± 0.3	13 ± 0.2	13 ± 0.1
LGNv	7 ± 0.2	8 ± 0.3	11 ± 0.1	9 ± 0.2
Shape factor:				
LGN	1.46 ± 0.02	1.44 ± 0.04	1.51 ± 0.03	1.82 ± 0.1
LGNd	1.44 ± 0.03	1.48 ± 0.04	1.46 ± 0.01	1.53 ± 0.01
LGNv	1.48 ± 0.01	1.40 ± 0.01	1.56 ± 0.02	2.12 ± 0.05

DISCUSSION

In all the examined species, the mean volume of the LGNd grew with the increase of the LGN volume. In the common shrew and the bank vole the percentage contribution of the LGNd to the total volume of the LGN is very similar (about 57–58%), whereas in the remaining two species it is considerably higher, reaching its highest value in the fox (95%). The simultaneous growth of the LGNv and LGN volumes was not so noticeable. In particular, it is noteworthy that the LGNv volume in the fox is three times smaller than that seen in the rabbit, despite the fact that the LGN volume in the fox is over two times larger than that of the rabbit. In comparison with the LGNd, the percentage contribution of the LGNv shows a reverse tendency, with the lowest value in the fox (5%). In the available literature, there are not many reports concerning the morphometric volumes of the LGN nuclei in different mammals. Only Brauer et al. [4] carried out complex research. They studied 16 species from 7 orders and estimated their LGNd/LGNv volume quotients. For example, the quotient in insectivores — 4.7 (hedgehog), rodents — from 1.4 to 2.7 (yellow-necked mouse and Brazilian guinea pig, respectively), leporids — from 2.7 to 4.1 (rabbit and brown hare, respectively), carnivores — from 17.4 to 24.1 (wildcat and least weasel, respectively), primates — from 27.8 to 107 (galago and human, respectively). The remaining existing data essentially concern the volume of the LGNd in a very limited number of species: the southern pig-tailed macaque (56.5 mm^3), the green monkey (32.38–39.43 mm^3), the marmoset monkey (10.71 mm^3), the cat (19.89 mm^3), the Gobi-Altai-Mountain vole (0.16 mm^3), and the silver grey mountain vole (0.23 mm^3) [2, 3, 9, 15, 19]. Interestingly, the LGNd volumes in the fox (present study) and cat [19] are nearly identical, while in the bank vole (present study) this parameter is similar to that of the house mouse [4] and both mountain voles [15]. Our results from the rabbit are similar to those of Brauer et al. [4]; however, slight differences could result from the fact that we investigated different breeds. Mammals with a high level of neocorticalization are characterized by a high quotient of LGNd and LGNv volumes [4]. This results from the different fibre connections of these two nuclei and the close relationship of the LGNd to the visual

cortex. The LGNd/LGNv quotient is exceptionally high in the human (107), especially when compared to other primates (about 30) [4]. In our study, this parameter was highest in the fox (20), which corresponds to other carnivores [4]. According to Brauer et al. [4] there is also a correlation between LGN volume and the occurrence of LGNd lamination, but only in members of the same order. The LGNv of most mammals comprises 2 main layers, which in some species can be further divided into sub-layers. In view of the Niimi et al. [25] comparative cytoarchitectural study, based on 12 species from 5 orders, the LGNv of ungulates is the most differentiated and developed, contrary to primate LGNv, which is the least developed. The authors [25] believe that LGNv is poorly developed in lower mammals, reaches its highest peak of phylogenetic development in ungulates, and reduces as the mammalian scale is ascended. Our results on the LGNv cytoarchitecture of rodents, leporids, and carnivores correspond to the data obtained by other authors [14, 23, 25]. It is also worth mentioning that only in primates is the LGNv situated dorsally to the LGNd; therefore, it is usually called the pregeniculate nucleus [1, 17, 18].

In the present study, the neuronal density of both LGN nuclei was generally negatively correlated with the volumes of the LGN as well as with brain size. The exception is the fox, which, despite having a larger volume of geniculate nuclei than the rabbit, has the higher number of neurons per mm^3. In all the examined species, the LGNv always had a higher numerical density than the LGNd, which clearly differentiated both nuclei. The decrease of the neuronal density with the simultaneous increase of the volume has been described in several different mammalian brain regions, namely the claustrum, amygdala, and lateral tuberal nucleus [16, 24, 26]. The literature on LGN numerical densities is scarce and concerns only the LGNd. There were from 27352 to 29334 neurons in 1 mm^3 of LGNd tissue in the green monkey, 32680 in the marmoset monkey, and 28183 in the cat [3, 9, 19]. All the above-mentioned species, similarly to the fox (present study), have a larger volume and at the same time a higher neuronal density of LGNd than the rabbit. This could imply that in the sensory brain centres the negative correlation between the volume and numerical density may not be as distinct as in the case of the non-sensory brain structures. The available data and present results seem to indicate that this type of correlation is impaired mainly in carnivores and primates. Members of other mammalian orders should not be excluded; however, this requires further and more detailed morphometric investigation.

In the present study, there was found to be a significant correlation between the volume and the mean neuronal population of both geniculate nuclei. A similar correlation was also noted in other brain areas [16, 24, 26]. The smallest number of neurons was observed in the common shrew, while the largest was seen in the fox, except for the rabbit LGNv, which had a higher neuronal population than the analogous nucleus in the fox. Despite the smaller density of LGNv in the rabbit, this nucleus outnumbers, in terms of neuronal population, the LGNv in the fox. This is because the volume of the rabbit LGNv is three times larger. The variability in the percentage contribution of the LGNd and LGNv cells to the total neuronal population of the LGN is similar to data regarding the percentages of volumes. The number of LGNd neurons was reported as 435900 in the marmoset monkey, 1790000 in the southern pig-tailed macaque, from 949835 to 1078489 in the green monkey, and from 545320 to 563080 in the cat [2, 3, 9, 19]. Analogously, as in the case of the other morphometric parameters, there is a strong resemblance between the fox and the cat. The fox LGNd has only a slightly larger volume, numerical density, and neuronal population than that of the cat.

The mean neuronal size of both geniculate nuclei, i.e. the resultant of the length, width, area, and circumference of the soma, grows correlatively to the volumes of these nuclei. The exceptions are LGNv cells in the rabbit and the fox, which have similar sizes. In the present study, the LGNd neurons of all species are distinctly larger than the LGNv cells. In addition, the somas of LGNd neurons in the studied species have more similar shapes than the LGNv perikarya. It is noteworthy that there is a striking discrepancy in the shape factor of the LGNv cells, between the fox and the remaining three species. This shows that in the fox LGNv, the spindle-shaped neurons are more numerous. In general, the growth of the sizes of geniculate cells in the studied species was not as high as the growth of neuronal populations and volumes, but it was systematic and noticeable.

Based on this study and other research reported in the literature, it can be seen that a significant disproportion is seen between the size of the LGNd and LGNv in carnivores and primates [1, 14, 18, 23, 25]. The species of these orders have LGNd that definitely surpass the LGNv in terms of size. Taking into consideration the fact that LGNv is believed to be mainly involved in visuomotor functions, an obvious question is raised

concerning the anatomical and physiological interpretation of such disproportion. Certainly, it can be safely assumed that any impairment of visuomotor coordination does not occur in these species. Presumably, the clearly larger size of the LGNd may be because carnivores and primates are highly visual mammals, also characterized by a high degree of neocorticalization. Comparative anatomy studies reveal that the highly organized visual system of primates has many features in common with that of carnivores [5, 12, 20, 27]. All species from these two orders, which have been examined so far, have a multilayered structure of the LGNd and have eyes positioned on the front of their heads, enabling binocular vision.

REFERENCES

1. Babb RS (1980) The pregeniculate nucleus of the monkey (Macaca mulatta). I. A study at the light microscopy level. J Comp Neurol, 190: 651–672.
2. Blasco B, Avendano C, Cavada C (1999) A stereological analysis of the lateral geniculate nucleus in adult Macaca nemestrina monkeys. Vis Neurosci, 16: 933–941.
3. Boire D, Théoret H, Ptito M (2002) Stereological evaluation of neurons and glia in the monkey dorsal lateral geniculate nucleus following an early cerebral hemispherectomy. Exp Brain Res, 142: 208–220.
4. Brauer K, Winkelmann E, Nawka S, Strnad W (1982) Comparative volumetric investigations on the lateral geniculate body of mammals. Z Mikrosk Anat Forsch, 96: 400–406.
5. Conley M, Birecree E, Casagrande VA (1985) Neuronal classes and their relation to functional and laminar organization of the lateral geniculate nucleus: a Golgi study of the prosimian primate, Galago crassicaudatus. J Comp Neurol, 242: 561–583.
6. Conley M, Friederich-Ecsy B (1993) Functional organization of the ventral lateral geniculate complex of the tree shrew (Tupaia belangeri): II. Connections with the cortex, thalamus, and brainstem. J Comp Neurol, 328: 21–42.
7. DeVito JL, Graham J, Sackett GP (1989) Volumetric growth of the major brain divisions in fetal Macaca nemestrina. Hirnforsh J, 30: 479–487.
8. Edelstein K, Amir S (1999) The role of the intergeniculate leaflet in entrainment of circadian rhythms to a skeleton photoperiod. J Neurosci, 19: 372–380.
9. Fritschy JM, Garey LJ (1986) Postnatal development of quantitative morphological parameters in the lateral geniculate nucleus of the marmoset monkey. Dev Brain Res, 30: 157–168.
10. Goel N, Governale MM, Jechura TJ, Lee TM (2000) Effects of intergeniculate leaflet lesions on circadian rhythms in Octodon degus. Brain Res, 877: 306–313.
11. Harrington ME (1997) The ventral lateral geniculate nucleus and the intergeniculate leaflet: interrelated structures in the visual and circadian systems. Neurosci Biobehav Rev, 21: 705–727.
12. Hassler R, Hajdu F (1985) Architectonic differentiation of the lateral geniculate body of the cat. J Hirnforsch, 26: 245–257.
13. Hickey TL, Spear PD (1976) Retinogeniculate projections in hooded and albino rats: An autoradiographic study. Exp Brain Res, 24: 523–529.
14. Higo S, Kawamura S (1999) Zonal organization of the ventral lateral geniculate nucleus in the cat: cholera toxin mapping. J Comp Neurol, 415: 17–32.
15. Hilbig H, Stubbe A, Winkelmann E (1989) Volumetric and golgi studies of the corpus geniculatum laterale pars dorsalis of Alticola stoliczkanus barakshin and Alticola argentatus semicanus. Z Mikrosk Anat Forsch, 103: 14–20.
16. Kowiański P, Dziewiątkowski J, Kowiańska J, Moryś J (1999) Comparative anatomy of the claustrum in selected species: a morphometric analysis. Brain Behav Evol, 53: 44–54.
17. Livingston CA, Fedder SR (2003) Visual-ocular motor activity in the macaque pregeniculate complex. J Neurophysiol, 90: 226–244.
18. Livingston CA, Mustari MJ (2000) The anatomical organization of the macaque pregeniculate complex. Brain Res, 876: 166–179.
19. Madarász M, Gerle J, Hajdu F, Somogyi Gy, Tömböl T (1978) Quantitative histological studies on the lateral geniculate nucleus in the cat II. Cell numbers and densities in the several layers. J Hirnforsch, 19: 159–164.
20. McConnell SK, Le Vay S (1986) Anatomical organization of the visual system of the mink, Mustela vison. J Comp Neurol, 250: 109–132.
21. Murphy PC, Duckett SG, Sillito AM (2000) Comparison of the laminar distribution of input from areas 17 and 18 of the visual cortex to the lateral geniculate nucleus of the cat. J Neurosci, 20: 845–853.
22. Najdzion J, Wasilewska B, Szteyn S, Robak A, Bogus-Nowakowska K, Równiak M (2006) The neuronal structure of the dorsal nucleus of the lateral geniculate body in the common shrew (Sorex araneus) and the bank vole (Clethrionomys glareolus): Golgi and Nissl studies. Folia Morphol, 65: 352–358.
23. Nakamura H, Itoh K (2004) Cytoarchitectonic and connectional organization of the ventral lateral geniculate nucleus in the cat. J Comp Neurol, 473: 439–462.
24. Narkiewicz O, Dziewíątkowski J, Moryś J (1994) Lateral tuberal nucleus in man and macaca comparative morphometric investigations. Folia Morphol, 53: 1–12.
25. Niimi K, Kanaseki T, Takimoto T (1963) The comparative anatomy of the ventral nucleus of the lateral geniculate body in mammals. J Comp Neurol, 121: 313–324.
26. Równiak M, Robak A, Szteyn S, Bogus-Nowakowska K, Wasilewska B, Najdzion J (2007) The morphometric study of the amygdala in the rabbit. Folia Morphol, 66: 44–53.
27. Tigges J, Tigges M (1987) Termination of retinofugal fibers and lamination pattern in the lateral geniculate nucleus of the gibbon. Folia Primatol, 48: 186–194.
28. Vrang N, Mrosovsky N, Mikkelsen JD (2003) Afferent projections to the hamster intergeniculate leaflet demonstrated by retrograde and anterograde tracing. Brain Res Bull, 59: 267–288.
29. West MJ, Gundersen HJ (1990) Unbiased stereological estimation of the number of neurons in the human hippocampus. J Comp Neurol, 296: 1–22.